Heliyon 10 (2024) e30269

Contents lists available at ScienceDirect

Heliyon

journal homepage: www.cell.com/heliyon

Research article

Identification of necroptosis-related diagnostic biomarkers in coronary heart disease

Hongjun You, Wenqi Han *

Department of Cardiovascular Medicine, Shaanxi Provincial People's Hospital, Xi'an, 710068, Shaanxi, China

ARTICLE INFO

Keywords:
Coronary heart disease
CHD
Necroptosis
Diagnosis
Immunity

ABSTRACT

Background: The implication of necroptosis in cardiovascular disease was already recognized. However, the molecular mechanism of necroptosis has not been extensively studied in coronary heart disease (CHD).

Methods: The differentially expressed genes (DEGs) between CHD and control samples were acquired in the GSE20681 dataset downloaded from the GEO database. Key necroptosis-related DEGs were captured and ascertained by bioinformatics analysis techniques, including weighted gene co-expression network analysis (WGCNA) and two machine learning algorithms, while single-gene gene set enrichment analysis (GSEA) revealed their molecular mechanisms. The diagnostic biomarkers were selected via receiver operating characteristic (ROC) analysis. Moreover, an analysis of immune elements infiltration degree was carried out. Authentication of pivotal gene expression at the mRNA level was investigated in vitro utilizing quantitative real-time PCR (qRT-PCR).

Results: A total of 94 DE-NRGs were recognized here, among which, FAM166B, NEFL, POLDIP3, PRSS37, and ZNF594 were authenticated as necroptosis-related biomarkers, and the linear regression model based on them presented an acceptable ability to different sample types. Following regulatory analysis, the ascertained biomarkers were markedly abundant in functions pertinent to blood circulation, calcium ion homeostasis, and the MAPK/cAMP/Ras signaling pathway. Single-sample GSEA exhibited that APC co-stimulation and CCR were more abundant, and aDCs and B cells were relatively scarce in CHD patients. Consistent findings from bioinformatics and qRT-PCR analyses confirmed the upregulation of NEFL and the downregulation of FAM166B, POLDIP3, and PRSS37 in CHD.

Conclusion: Our current investigation identified 5 necroptosis-related genes that could be diagnostic markers for CHD and brought a novel comprehension of the latent molecular mechanisms of necroptosis in CHD.

Abbreviations: CHD, coronary heart disease; DEGs, differentially expressed genes; WGCNA, weighted gene co-expression network analysis; GSEA, gene set enrichment analysis; ROC, receiver operating characteristic; qRT-PCR, quantitative real-time PCR; GEO, Gene Expression Omnibus; FC, fold change; NRGs, necroptosis-related genes; GO, Gene Ontology; KEGG, Kyoto Encyclopedia of Genes and Genomes; SVM, Support Vector Machine; RFE, recursive feature elimination; AUC, area under the curve; NES, Normalized Enrichment Score; PBMC, peripheral blood mononuclear cell.

* Corresponding author.
E-mail address: hwq315@163.com (W. Han).

https://doi.org/10.1016/j.heliyon.2024.e30269
Received 3 June 2023; Received in revised form 12 April 2024; Accepted 23 April 2024
Available online 25 April 2024

1. Introduction

A cardiovascular disease predominantly featured by impaired coronary artery blood supply, coronary heart disease (CHD), is globally one of the most common chronic non-communicable diseases. As the demographic ages and the prevalence of poor lifestyles, the incidence and mortality of CHD trend upward [1]. As per a recent release from the World Health Organization, the prevalence of CHD has increased from 27.3 % to 31.4 % in the past decades [2]. The China Cardiovascular Health and Disease Report 2021 indicated that the prevalence of CHD in China was about 11.0 %. Furthermore, urban residents have experienced a mortality rate of 121.59 deaths per 100,000 due to CHD, while rural residents have seen a rate of 130.14 deaths per 100,000 [3]. These data demonstrate the serious burden of the disease on global health.

Frequent risk factors for CHD have been described, ranging from hypertension, hyperlipidemia, diabetes, obesity, smoking, lack of exercise, and familial inheritance [4]. Although therapeutic measures including medications and surgery in CHD have been extensively utilized [5,6], there are still limitations and drawbacks, such as difficulty in curing the disease, poor treatment outcomes in patients with high-risk factors, and postoperative complications. Modifications of multiple genes and signaling pathways were demonstrated to be responsible for controlling CHD progression [7]. However, the lack of precise molecular mapping studies of the CHD process may limit the renovation of existing diagnostic and management paradigms for the disease.

Necroptosis is a novel kind of programmed cell death with characteristics of both necrosis and apoptosis [8]. Previous studies have pointed out that necroptosis features an essential character in the immune system, inflammatory response, and the onset and progression of several diseases [9,10]. Necroptosis has been implicated in the pathogenesis and development of cardiovascular diseases, such as atherosclerosis, myocardial infarction, and abdominal aortic aneurysm, which may be related to RIP3 [11]. In CHD progression, necroptosis is ascribed as a critical element in plaque formation, stability, and rupture [12,13]. Moreover, necroptosis may also trigger an inflammatory response [14], exacerbating CHD progression and deleterious outcomes. Currently, however, the genetic landscape related to necroptosis in CHD is not well-established. Presently, the CHD-based genetic landscape associated with necroptosis is urgently needed to be elucidated.

In this study, we dissected a dataset extracted from the GEO database (GSE20681) containing samples from CHD (n = 99) and paired healthy individuals (n = 99) to characterize the CHD-related DEGs. Further, WGCNA and superposition analysis were employed to figure out the necroptosis-related DEGs in CHD. Machine learning algorithms were followed to ascertain the critical biomarkers and elucidate the biological functions of these genes via functional richness analysis. Additionally, we verified the critical biomarkers further by subject ROC analysis and RT-PCR analysis. The achievements of this study potentially point to innovative perspectives on therapeutic targets for CHD in necroptosis.

2. Materials and methods

2.1. Information retrieval

The RNA-seq data of whole blood cells from 99 CHD patients and 99 control samples were extracted from the GSE20681 dataset (https://www.ncbi.nlm.nih.gov/geo/query/acc.cgi?acc=GSE20681) obtained from the Gene Expression Omnibus (GEO) database. The 159 necroptosis genes (Table 1) identified in the hsa04217 pathway were sourced from the Kyoto Encyclopedia of Genes and Genomes (KEGG) database.

2.2. Necroptosis score

The necroptosis score was computed for each sample in the GSE20681 dataset using the GSVA package (version 1.42.0) [15] via the single-sample gene set enrichment analysis (ssGSEA) algorithm. All samples were to be partitioned into high- and low-necroptosis scoring groups depending on the median necroptosis score (median = 0.428), and details of the scores and groupings as reviewed in Supplementary Table 1.

Table 1
159 necroptosis genes extracted from hsa04217 pathway.

Necroptosis genes
TNF, TNFRSF1A, TRADD, TRAF2, TRAF5, RIPK1, BIRC2, BIRC3, XIAP, RBCK1, RNF31, SHARPIN, SPATA2L, SPATA2, CYLD, FADD, CASP8, CFLAR, RIPK3, CYBB, CAMK2A, CAMK2D, CAMK2B, CAMK2G, SLC25A4, SLC25A5, SLC25A6, SLC25A31, PPID, VDAC1, VDAC2, VDAC3, GLUD2, GLUD1, GLUL, PYGL, PYGM, PYGB, MAPK8, MAPK10, MAPK9, FTH1, FTL, PLA2G4E, PLA2G4A, JMJD7-PLA2G4B, PLA2G4B, PLA2G4C, PLA2G4D, PLA2G4F, ALOX15, CAPN1, CAPN2, SMPD1, MLKL, PGAM5, DNM1L, NLRP3, PYCARD, CASP1, IL1B, CHMP2A, CHMP2B, CHMP3, RNF103-CHMP3, CHMP4B, CHMP4A, CHMP4C, CHMP6, VPS4B, VPS4A, CHMP1B, CHMP1A, CHMP5, CHMP7, TRPM7, IL1A, IL33, HMGB1, TNFSF10, TNFRSF10A, TNFRSF10B, FASLG, FAS, FAF1, IFNA1, IFNA2, IFNA4, IFNA5, IFNA6, IFNA7, IFNA8, IFNA10, IFNA13, IFNA14, IFNA16, IFNA17, IFNA21, IFNB1, IFNG, IFNAR1, IFNAR2, IFNGR1, IFNGR2, JAK1, JAK2, JAK3, TYK2, STAT1, STAT2, STAT3, STAT4, STAT5A, STAT5B, STAT6, IRF9, EIF2AK2, TLR4, TICAM2, TICAM1, TLR3, ZBP1, USP21, SQSTM1, HSP90AA1, HSP90AB1, TNFAIP3, PARP1, BID, BAX, AIFM1, H2AX, H2AC20, H2AC12, H2AC1, H2AC25, H2AB3, H2AC8, H2AC4, MACROH2A2, MACROH2A1, H2AC19, H2AJ, H2AB1, H2AC17, H2AC18, H2AC11, H2AC21, H2AZ2, H2AC7, H2AZ1, H2AC15, H2AC6, H2AC13, H2AC14, H2AC16, H2AB2, PPIA, BCL2

2.3. Filtering for key module genes by WGCNA

Utilizing WGCNA package (version 1.71) [16], we performed WGCNA analysis based on RNA sequencing data from the GSE20681 dataset. The necroptosis score was the specific trait of interest in this study. Briefly, first, we assessed the correlation of all samples included (CHD: 99; healthy controls: 99) by cluster analysis. Based on outlier characteristics, we excluded samples GSM518964, GSM519036, and GSM519070 (healthy control group) from consideration in subsequent WGCNA analyses to ensure the reliability of the results. Subsequently, the adjacency matrix was utilized to construct a co-expression network that followed a scale-free topology, employing a soft-thresholding parameter β. Importantly, this parameter served to amplify strong correlations between genes while simultaneously downplaying weaker associations, thus enhancing the network's overall cohesiveness [17]. Next, to group genes exhibiting comparable expression profiles, we executed a hierarchical clustering analysis with the aim of identifying modules, each characterized by no fewer than 30 genes (minModuleSize = 30). Then, similar modules were merged according to mergeCutHeight = 0.3. Ultimately, we checked out the connections between modules and phenotypic traits, subsequently electing the module displaying a |correlation coefficient (cor)| exceeding 0.3 and a *P*-value under 0.05 as the module of interest and labeled the genes inside it as necroptosis-related genes (NRGs).

2.4. Analysis of differential expression

Based on the defined significance threshold: $|\log_2$ fold change (FC)$| > 0$ and $P < 0.05$, CHD-related DEGs were confirmed by R package limma (version 3.50.3) [18] in the CHD group (n = 99) vs. healthy control group (n = 99). The volcano map was drawn with the ggplot2 package (version 3.3.6) [19], and employed the pheatmap package (version 1.0.12) [20] to generate the heatmap.

2.5. Recognition of duplicated elements

We utilized the Jvenn online tool [21] to conduct Venn diagram analysis in order to identify the overlap between the CHD-related DEGs and the NRGs list, which we defined as DE-NRGs.

2.6. Function annotation

The potential biological processes of the identified DE-NRGs were annotated by Gene Ontology (GO) and the Kyoto Encyclopedia of Genes and Genomes (KEGG) analysis in the R-based clusterProfiler package (version 3.14.3), which can search for common functions of many genes and related pathways within the target gene set [22,23].

2.7. Machine learning algorithms

In this study, we leveraged two distinct machine learning approaches - LASSO algorithm and SVM-RFE algorithm - to sift for characteristic genes in the GSE20681 dataset. LASSO Cox regression, a popular approach for selecting high-dimensional predictors, was implemented in this study using the glmnet (version 4.1–4) package [24]. The parameters were set to family = 'binomial', type. measure = 'class', nfold = 10, which means 10-fold cross-validation. We produced a cross-validation fit plot and determined the threshold value for lambda (λmin) as the minimum point on the curve. Support Vector Machine (SVM) is a supervised learning approach that serves as a generalized linear classifier, optimizing the margin between different classes in a high-dimensional space during the binary classification of data [25]. The above DE-NRGs were screened for feature genes by the SVM algorithm using R package e1071 (version 1.7–11) [26]; then, the importance and ranking of each gene were obtained using the recursive feature elimination (RFE) method (specifically, RFE refers to the iterative process of gradually reducing from the combination of all input genes to one gene combination, calculating the importance ranking of each iteration, and removing the unimportant genes, using the remaining genes to rank the importance again, and so on); meanwhile, the error rate of each combination of iterations was collated; finally, the best gene combination with the lowest error rate was selected, and the corresponding gene was extracted as the signature gene.

Concurrently applying the two machine learning algorithms, we performed a gene screening process that allowed us to identify a set of key genes (referred to as necroptosis-related biomarkers), which were obtained through Venn analysis. Then, we constructed a ROC and calculated the area under the curve (AUC) to estimate the predictive value of the critical biomarkers. Afterthat, the linear regression model was constructed based on the necroptosis-related biomarkers to differentiate normal and CHD samples using biomarkers as a whole.

2.8. Single-gene GSEA analysis of biomarkers

To determine the enriched regulatory pathways and biological functions of each necroptosis-related biomarker, we implemented single-gene GSEA using clusterProfiler package (version 3.14.3). We only considered gene sets with |Normalized Enrichment Score (NES)| > 1, adjusted (adj.) $P < 0.05$, and $q < 0.25$ as significant. The top 5 results for GO and KEGG significance were visualized separately.

2.9. Immuno-infiltration and correlation analysis

We utilized the ssGSEA approach available in the gsva R package [27] to evaluate the infiltrating status of 29 immune elements. Moreover, we conducted a Pearson correlation analysis to explore the association between immune cells and essential biomarkers.

2.10. Clinical specimen collection

Fasting whole blood samples were collected from ten patients diagnosed with CHD and ten healthy volunteers without clinical evidence of CHD, and their clinical characteristics were exhibited in Table 2. These samples were obtained from the left median cubital vein and stored at −80 °C for subsequent experimentation. All CHD patients were obtained from in the Shaanxi Provincial People's Hospital, Xi'an, Shaanxi, China. Approval for conducting the study was obtained from the Ethics Review Committee of the hospital, and written informed consent was acquired from all patients before their participation in the study.

2.11. RNA isolation and quantitative real-time polymerase chain reaction (qRT-PCR)

The peripheral blood mononuclear cell (PBMC) separation solution with the same volume of blood was added to the centrifuge tube, and centrifuged at 2000g for 20 min to obtain PBMC located in the second layer. Then, TRIzol reagent was used to lyse the PBMCs and total RNA was extracted in accordance with the instructions provided by the manufacturer. The concentration of RNA was measured with a NanoPhotometer N50. For cDNA synthesis, the SureScript First strand cDNA synthesis kit (Servicebio, Wuhan, China) was utilized to reverse transcribe the extracted RNA. The qRT-PCR reaction involved combining 3 μL of the reverse transcription product with 5 μL of 2xUniversal Blue SYBR Green qPCR Master Mix, as well as 1 μL each of the forward and reverse primers. All primer sequence information were shown in Table 3. To determine the relative expression of genes, we used the $2^{-\Delta\Delta CT}$ method [28], with the GAPDH gene serving as an internal control. Statistical analysis was carried out using unpaired t-tests, using GraphPad Prism V6 (GraphPad Software, La Jolla, CA, USA) to compare the expression of 5 key mRNAs between normal and CHD samples. Results were reported as * for $P < 0.05$ and ** for $P < 0.01$ to indicate statistical significance.

2.12. Statistical analysis

All bioinformatics analyses were undertaken in R language. Significance was set at $P < 0.05$, unless specified otherwise.

3. Results

3.1. Identification of key module associated with necroptosis scores in the GSE20681 dataset

To identify the key module strongly associated with necroptosis scores, WGCNA was performed on the expression profile of 198 samples in the GSE20681 dataset. The co-expression modules' mean connectivity followed a scale-free network distribution in accordance with a soft threshold power of $\beta = 13$ (scale-free $R^2 = 0.90$), as illustrated in Supplementary Fig. 1A. Upon cluster merging, we identified sixteen modules composed of genes with similar connection strength patterns to other genes (Supplementary Fig. 1B). Based on the relationship heatmap between modules and necroptosis score traits, the MEorange (|cor| = 0.39, P = 2e-08), MEblue (|

Table 2
Clinical characteristics of clinical samples used for PCR analysis.

Group	Disease status	Gender	Age	Ethnicity
Control 1	healthy volunteer	male	77	Chinese, xanthoderm
Control 2	healthy volunteer	male	66	Chinese, xanthoderm
Control 3	healthy volunteer	male	76	Chinese, xanthoderm
Control 4	healthy volunteer	female	60	Chinese, xanthoderm
Control 5	healthy volunteer	male	59	Chinese, xanthoderm
Control 6	healthy volunteer	female	66	Chinese, xanthoderm
Control 7	healthy volunteer	male	50	Chinese, xanthoderm
Control 8	healthy volunteer	male	49	Chinese, xanthoderm
Control 9	healthy volunteer	male	69	Chinese, xanthoderm
Control 10	healthy volunteer	male	64	Chinese, xanthoderm
CHD 1	acute myocardial infarction	male	54	Chinese, xanthoderm
CHD 2	acute myocardial infarction	male	71	Chinese, xanthoderm
CHD 3	acute myocardial infarction	male	59	Chinese, xanthoderm
CHD 4	acute myocardial infarction	female	69	Chinese, xanthoderm
CHD 5	acute myocardial infarction	male	38	Chinese, xanthoderm
CHD 6	acute myocardial infarction	male	50	Chinese, xanthoderm
CHD 7	acute myocardial infarction	male	52	Chinese, xanthoderm
CHD 8	acute myocardial infarction	male	82	Chinese, xanthoderm
CHD 9	acute myocardial infarction	male	54	Chinese, xanthoderm
CHD 10	acute myocardial infarction	female	76	Chinese, xanthoderm

Table 3
qRT-qPCR primers for genes.

Gene	Primer sequence	
FAM166B	Forward	CATGTCAGGCTTCACTGGCTAT
	Reverse	GTGCTTCTGCCCAAATTCCT
NEFL	Forward	CTGGAAATCGAAGCATGCCG
	Reverse	GCGGGTGGACATCAGATAGG
POLDIP3	Forward	TTAATGCCAGACCGGGAGTT
	Reverse	CACAGGGTCCACATGCATTCT
PRSS37	Forward	CCTGCTCCCTATTTGGTGTACC
	Reverse	CGGACGATCTGAATGGGGT
ZNF594	Forward	GACCGCAGGAGGATGTAGGC
	Reverse	TACCCACAGGAGGGAACTGG
GAPDH	Forward	CGAAGGTGGAGTCAACGGATTT
	Reverse	ATGGGTGGAATCATATTGGAAC

cor| = 0.37, P = 9e-08), and MElightyellow (|cor| = 0.35, P = 5e-07) modules were tightly linked to necroptosis scores (Supplementary Fig. 1C), which were considered as key modules of interest to be explored in subsequent analyses. Collectively, a total of 4794 NRGs (Supplementary Table 2) were extracted from the MEorange (1255 modular genes), MEblue (3007 modular genes), and MElightyellow (532 modular genes) modules.

3.2. Recognition of DE-NRGs in CHD patients

To identify the DEGs between the CHD patients and healthy samples, we comprehensively analyzed the gene expression microarray dataset obtained from the GSE20681 dataset. There were 859 DEGs in CHD patients compared with healthy samples, of which 548 were up-regulated and 311 were down-regulated (Fig. 1A, Supplementary Table 3). To further identify the DEGs strongly associated with necroptosis, we combined the NRGs with DEGs. The Venn diagram illustrated 94 intersecting genes between DEGs and NRGs (Fig. 1B), which were defined as DE-NRGs (up-regulated: 26, down-regulated: 68; Fig. 1C; Table 4), for subsequent analysis.

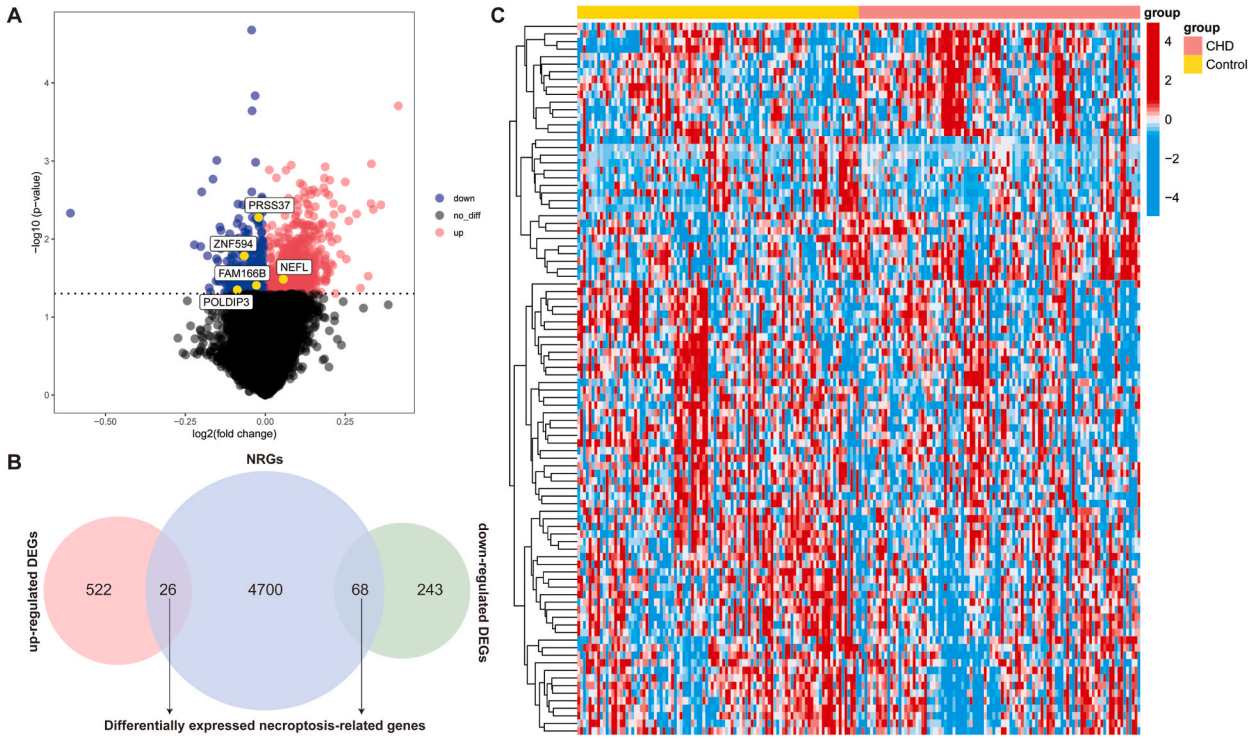

Fig. 1. Differentially expressed necroptosis-related genes (DE-NRGs) in CHD patients (CHD group) and healthy individuals (Control group). A. Volcano plot of 859 differentially expressed genes (DEGs). The red dots in the picture represent significantly up-regulated genes, blue dots represent significantly down-regulated genes, black dots represent genes that are not differentially expressed, and the five biomarkers identified in this study are marked. B. In the Venn diagram of DEGs and NRGs, the intersection part is considered as DE-NRGs. C. The heatmap of 94 DE-NRGs. Red represents up-regulated genes and blue represents downregulated genes. CHD, coronary heart disease.

Table 4
Expression of the identified 94 DE-NRGs in the GSE20681 dataset.

Gene name	Changed
HIST2H2BD, JADE1, HSPA1A, HERPUD1, MAN2A2, HIST1H2AD, ARFGAP3, NEFL, RLIM, HIST1H3B, NRDC, HIST1H3D, LASP1, NEU1, HIST3H2A, FAM212B, MOSPD3, CASC2, MAGEC1, F11R, SAP30, IGLON5, ATXN1, SERINC1, HEIH, DUSP9	up
CD83, CYP2U1, PRSS37, MEIG1, TRMT61A, LOC145783, DDX51, ILF3, DZIP3, ELK4, FCMR, FAM117B, SLC25A32, CHD6, ZNF235, ZNF594, SLC7A6, SPIN4, LOC286191, THAP9, EVL, NSMF, C1orf228, HLA-DPA1, OR12D2, PCED1B, WNT10B, SCML1, SFXN2, ATP9B, FAM221A, ARHGEF19, IGSF8, BRAT1, AES, KLRB1, ZNF550, CEP57, LOC101929147, ST6GAL1, HSF2, APOBEC3C, IDUA, 2-Mar, DDX39A, FAM166B, SMPD2, C1orf35, PRMT7, FLT3LG, PPRC1, NT5E, ACSF2, ADGRA3, MCM7, INTS6L, ZNF879, POLDIP3, CSF3, CHCHD10, CLINT1, ZNF526, C1orf159, KLF12, FMR1NB, TMC8, ABLIM1, MYC	down

3.3. Functional enrichment analysis on DE-NRGs

Potential functions of 94 DE-NRGs were predicted using GO and KEGG pathway analysis. Following $P < 0.05$, the enrichment analysis revealed that DE-NRGs were addressed in a total of 115 BP items, 14 CC items, 26 MF items (Supplementary Table 5 (Sheet 1)), and 9 KEGG pathways (Supplementary Table 4 (Sheet 2)). The top 10 enrolled in the GO-BP category were displayed in Fig. 2A, indicating that these DE-NRGs were specifically relevant to the endoplasmic reticulum stress-/mitochondrial outer membrane permeability-induced/involved apoptosis ('negative regulation of endoplasmic reticulum stress-induced intrinsic apoptotic signaling pathway', $P = 0.002722$; 'regulation of mitochondrial outer membrane permeabilization involved in apoptotic signaling pathway', $P = 0.003001$; 'regulation of endoplasmic reticulum stress-induced intrinsic apoptotic signaling pathway', $P = 0.006895$). Meanwhile, GO results hinted that DE-NRGs may serve molecular functions such as 'ATP hydrolysis activity' ($P = 0.003083$), 'helicase activity' ($P = 0.00386$), and 'hydrolase activity, hydrolyzing O-glycosyl compounds' ($P = 0.006902$) (Fig. 2B) in mitochondrial membrane components ('intrinsic component of mitochondrial inner membrane', $P = 0.020059$; 'integral component of mitochondrial inner membrane', $P = 0.020059$; 'integral component of mitochondrial membrane', $P = 0.045126$; 'intrinsic component of mitochondrial membrane'; $P = 0.046061$) (Fig. 2C). KEGG enrichment analysis disclosed the most pronounced enrichment in the 'MAPK signaling pathway' ($P = 0.004542$; count = 5) (Fig. 2D). Consistently, GO-BP highlighted that these genes were abundant in the 'negative regulation of MAPK cascade' (P = 0.033288), which may provide additional molecular evidence that necroptosis controls CHD by participating in the regulation of the MAPK signaling pathway.

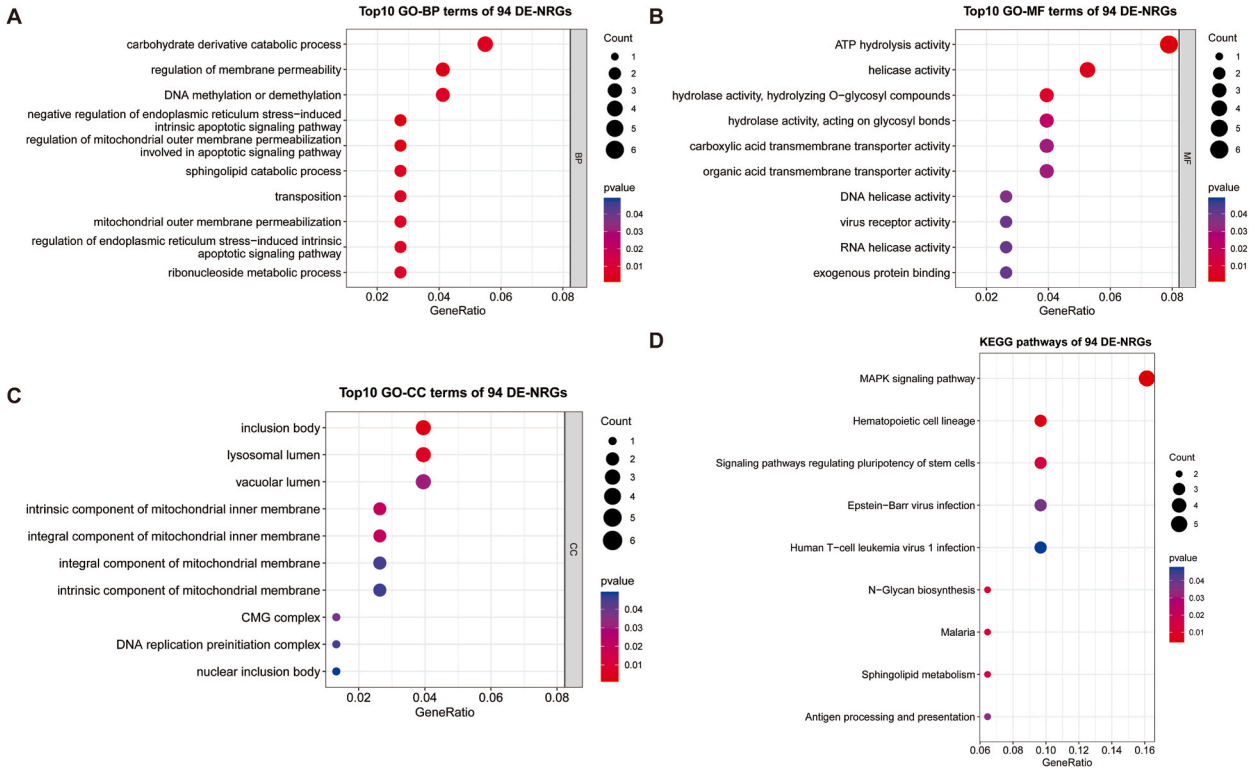

Fig. 2. GO and KEGG analyses of differentially expressed necroptosis-related genes (DE-NRGs) in CHD samples. GO-BP (A), -MF (B), and –CC (C) analysis for the major targets of DE-NRGs. D. KEGG analysis for the major targets of DE-NRGs. CHD, coronary heart disease; BP, biological process; CC, cellular component; MF, molecular function.

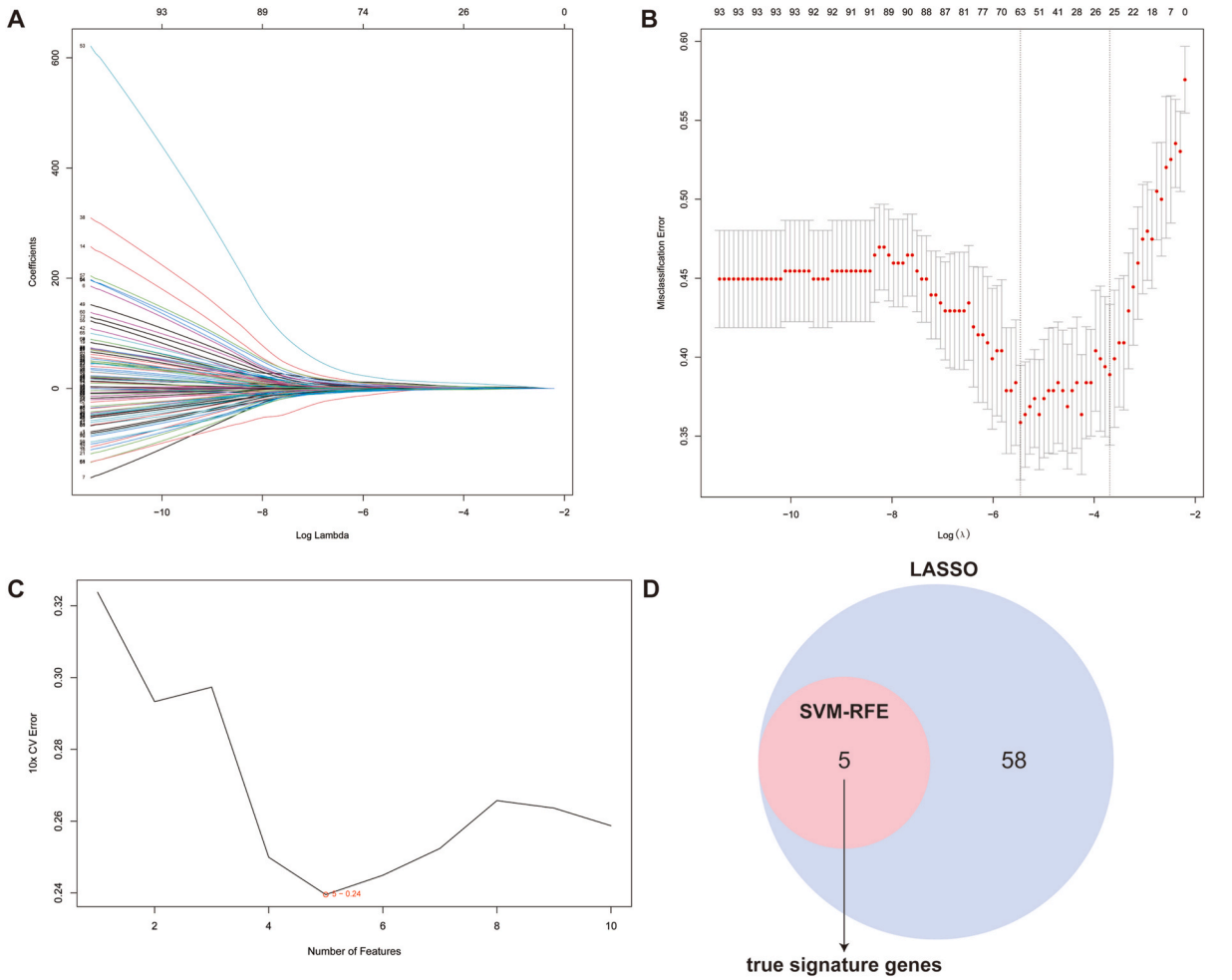

(caption on next page)

Fig. 3. Screening and assessment of the diagnosis-related DE-NRGs A. Tenfold cross-validation for tuning parameter selection in the LASSO model. B. LASSO coefficient profiles of 63 diagnostic DE-NRGs for CHD. C. The error rate of the estimate generation for the SVM-RFE algorithm. D. The intersection feature selection between LASSO and SVM-RFE algorithms. Evaluation of the prediction efficiency of the 5 signature genes (E) and the linear regression model (F) using ROC analysis in GSE20681. DE-NRGs, differentially expressed necroptosis-related genes; CHD, coronary heart disease; LASSO, least absolute shrinkage and selection operator; SVM-RFE, support vector machine recursive feature elimination.

3.4. Identification and evaluation of necroptosis-related biomarkers

To obtain the key biomarkers for CHD, we used two machine learning algorithms, LASSO and SVM-RFE, to downscale 94 DE-NRGs in the GSE20681 dataset. In the LASSO regression analysis, 63 signature genes were screened by the ten-fold cross-validation method based on $\lambda_{min} = 0.004$ (Fig. 3A and B; Table 5). Meanwhile, the SVM-RFE combined with the ten-fold cross-validation screened 5 signature genes (*FAM166B*, *NEFL*, *POLDIP3*, *PRSS37*, and *ZNF594*), at which point the SVM-RFE model had the lowest error rate (error rate = 0.24) (Fig. 3C). Finally, we combined the results of the two machine-learning algorithms and identified a total of five true signature genes, namely *FAM166B*, *NEFL*, *POLDIP3*, *PRSS37*, and *ZNF594* (Fig. 3D).

Then, we evaluated the ability of the above five signature genes to distinguish CHD and healthy control samples by ROC curve analysis in the GSE20681 dataset. The results were shown in Fig. 3E, and the 5 signature genes were not satisfactory in identifying sample types with all AUC <0.6. However, the linear regression model based on these 5 signature genes had an AUC of 0.75 in the GSE20681 dataset (Fig. 3F), indicating the satisfactory ability of the 5-gene model in distinguishing CHD samples from healthy control samples. This evidence suggested that five signature genes were of potential diagnostic value and they were defined as necroptosis-related biomarkers for subsequent analysis.

3.5. Exploring the potential molecular mechanisms of the necroptosis-related biomarkers

We revealed the potential biological pathways of the necroptosis-related biomarkers by single-genes GSEA. In the GO analysis, *FAM166B* was enriched in a total of 861 GO terms (BP: 566, CC: 140, MF: 155; Supplementary Table 5 (Sheet1)); *NEFL* was enclosed in a total of 1131 GO terms (BP: 803, CC: 174, MF: 154; Supplementary Table 5 (Sheet2)); *POLDIP3* was enrolled in 658 GO terms (BP: 425, CC: 118, MF: 115; Supplementary Table 5 (Sheet3)); *PRSS37* was involved in a total of 1024 GO terms (BP: 665, CC: 176, MF: 183; Supplementary Table 5 (Sheet4)); *ZNF594* was enriched to a total of 1272 GO terms (BP: 881, CC: 194, MF: 197; Supplementary Table 5 (Sheet5)). Fig. 4 presented the principal five GO terms associated with *FAM166B* (Fig. 4A), *NEFL* (Fig. 4B), *POLDIP3* (Fig. 4C), *PRSS37* (Fig. 4D), and *ZNF594* (Fig. 4E). In this study, we concentrated on these biomarker-enriched GO-BP terms. The combined analysis revealed that they were jointly enriched for a total of 178 BP terms (Supplementary Table 6), among which, interestingly, blood circulation ('blood circulation', 'regulation of blood circulation', and 'regulation of systemic arterial blood pressure'), membrane potential ('regulation of membrane potential', 'regulation of postsynaptic membrane potential', 'action potential', etc.), catecholamine regulation ('catecholamine transport', 'catecholamine secretion', 'regulation of catecholamine secretion', etc.), and calcium regulation ('cellular calcium ion homeostasis', 'calcium ion transport into cytosol', 'regulation of calcium ion transport', etc.) were significantly enriched; additionally, 'cell-cell adhesion via plasma-membrane adhesion molecules', 'positive regulation of MAPK cascade', and 'somatic diversification of immune receptors' were also tightly linked to the identified biomarkers.

KEGG analysis was also performed by GSEA against individual necroptosis-related biomarkers to reveal the pathways in which they were involved. *FAM166B* was involved in a total of 51 KEGG pathways (Supplementary Table 7 (Sheet1)), *NEFL* was significantly associated with 102 KEGG pathways (Supplementary Table 7 (Sheet2)), *POLDIP3* was enriched for a total of 76 pathways (Supplementary Table 7 (Sheet3)), *PRSS37* was related to 54 KEGG pathways (Supplementary Table 7 (Sheet4)), and ZNF594 was involved in 60 pathways (Supplementary Table 7 (Sheet5)). The comprehensive analysis highlighted that all these necroptosis-related biomarkers were engaged in pathways associated with cardiac disease progressions, such as the 'cAMP signaling pathway', 'Calcium signaling pathway', and 'Ras signaling pathway'; meanwhile, these genes were also intimately correlated with 'Dilated cardiomyopathy'. Fig. 5 depicted the five foremost pathways linked with *FAM166B* (Fig. 5A), *NEFL* (Fig. 5B), *POLDIP3* (Fig. 5C), *PRSS37* (Fig. 5D), and *ZNF594* (Fig. 5E). In conclusion, we believe that the above significantly enriched pathway enriched by biomarkers will inform further exploration of its potential mechanism of action in CHD.

3.6. Intergroup differences in immune elements and correlation with biomarkers

We evaluated the abundance of immune infiltrating elements in 99 CHD and 99 healthy control samples from the GSE20681 dataset by means of ssGSEA. Using the Wilcoxon rank sum test, we observed significantly higher levels of APC co-stimulation and CCR in the

Table 5
List of 63 signature genes screened by LASSO.

LASSO signature genes
HIST2H2BD, SCML1, JADE1, SLC7A6, OR12D2, HSPA1A, CYP2U1, PRMT7, ACSF2, HSF2, FAM166B, HEIH, F11R, SAP30, ILF3, CHD6, CD83, SPIN4, AES, DZIP3, SLC25A32, CLINT1, SFXN2, DUSP9, INTS6L, HLA-DPA1, LOC145783, ZNF235, KLRB1, C1orf159, HERPUD1, TMC8, ATP9B, FAM221A, LOC286191, DDX39A, ADGRA3, FCMR, PRSS37, MEIG1, ZNF594, MARC2, POLDIP3, FAM117B, TRMT61A, ABLIM1, LOC101929147, PCED1B, NEFL, RLIM, IDUA, ATXN1, CHCHD10, C1orf228, HIST1H3B, NRDC, NSMF, IGSF8, ARHGEF19, FLT3LG, FAM212B, MOSPD3, THAP9

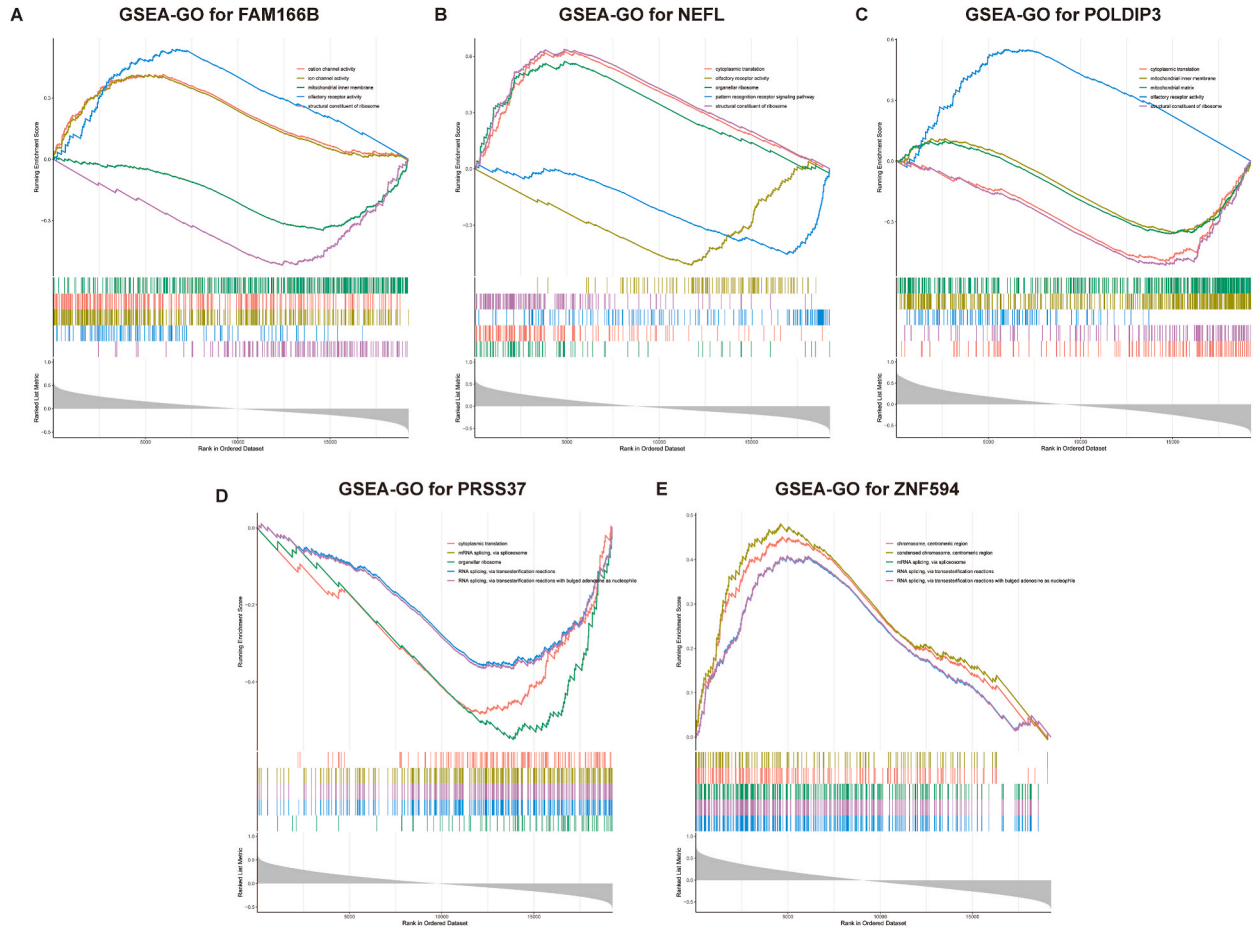

Fig. 4. Single gene GSEA-GO for the 5 necroptosis-related biomarkers. Enrichment in GO collection by FAM166B (A), NEFL (B), POLDIP3 (C), PRSS37 (D), and ZNF594 (E). Each line represents one gene set with unique color. Gene sets were considered significant only when $|NES| > 1$, $P < 0.05$, and $q < 0.05$. Only several leading gene sets (Top 5) were displayed in the plot. GSEA, gene set enrichment analysis; GO, Gene Ontology; NES, normalized enrichment score.

CHD group compared to the healthy control group, while aDCs and B cells were more prevalent in the latter (Fig. 6A). Next, we computed the Pearson correlation coefficients between 5 necroptosis-related biomarkers and the four immune infiltrating elements that exhibited significant differential abundances as previously described. The results were shown in Fig. 6B. *ZNF594* exhibited a significant moderate negative relationship with CCR (cor = −0.50745, $P = 2.35e\text{-}4$) and a weak positive association with B cells (cor = 0.30665, $P = 1.11e\text{-}5$); *POLDIP3* had a weak negative association with aDCs (cor = −0.33743, $P = 1.17e\text{-}6$) (Table 6). Moreover, the heat map of the correlation between immune infiltrating elements was displayed in Fig. 6C. Analysis of the four elements with differential abundance revealed that B cells had a weak positive correlation with aDCs (cor = 0.374868, $P = 6.71e\text{-}8$) and a weak negative interaction with CCR (cor = −0.30993, $P = 9.82e\text{-}6$). Detailed information on the results of the correlation analysis between all elements was retrieved in Supplementary Table 8. Therefore, we hypothesized that alterations in the immune microenvironment may play an important role in the developmental process of CHD, and in particular, the four differential immune cells may provide new insights in the search for therapeutic targets for CHD.

3.7. Validation of necroptosis-related biomarkers by qRT-PCR

In order to further verify the expression of necroptosis-related biomarkers, we conducted qRT-PCR experiments using clinical samples. The results depicted in Fig. 7 demonstrate a significant increase in mRNA levels of *NEFL* in the CHD group compared to the normal group (Fig. 7A; $P < 0.01$), and a marked decrease in mRNA levels of *FAM166B* and *POLDIP3* in the CHD group (Fig. 7B and C; $P < 0.05$). These findings were consistent with our bioinformatic analysis and provide additional evidence to support the role of necroptosis in CHD. Furthermore, although the mRNA levels of *PRSS37* were not statistically significant between the CHD and normal groups, a downward trend consistent with bioinformatic analysis was still detected (Fig. 7D). However, discordantly, qRT-PCR signaled that mRNA levels of *ZNF594* were seriously upregulated in the CHD group (Fig. 7E; $P < 0.05$), which may be explained by the heterogeneity of the samples.

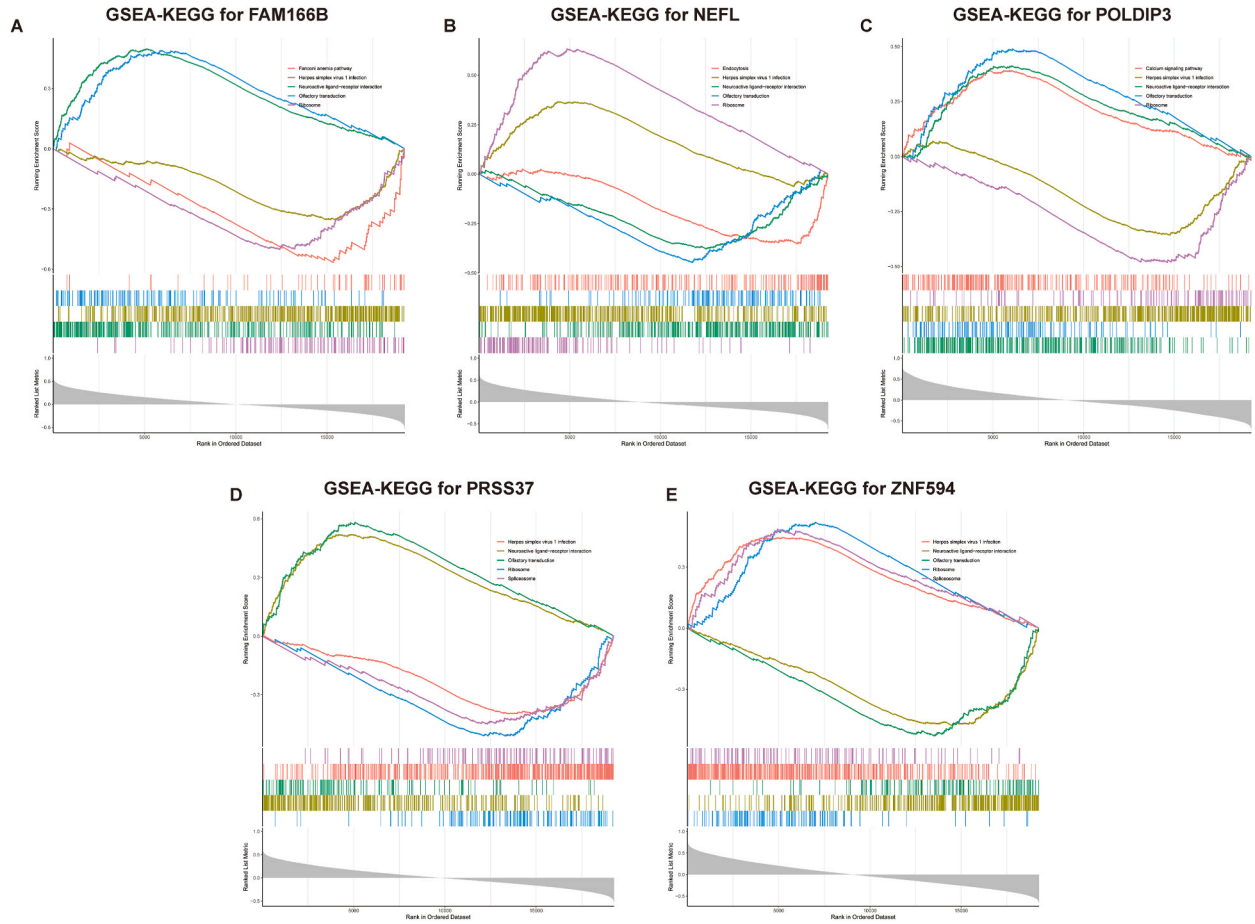

Fig. 5. Single gene GSEA-KEGG for the 5 necroptosis-related biomarkers. The enriched gene sets in KEGG collection by FAM166B (A), NEFL (B), POLDIP3 (C), PRSS37 (D), and ZNF594 (E). Each line represents one gene set with unique color. Only gene sets with $|NES| > 1$, $P < 0.05$, and $q < 0.05$ were considered significant. Only several leading gene sets (Top 5) were displayed in the plot. GSEA, gene set enrichment analysis; KEGG, Kyoto Encyclopedia of Genes and Genomes; NES, normalized enrichment score.

4. Discussion

Although substantial progress has been made in exploring the progression of CHD [29], with inflammatory factors such as C-reactive protein and interleukin-6 (IL-6) receiving the limelight [30,31], however, the clinically available therapeutic strategies have failed to prevent or reverse the cardiac injury [32,33]. Noticeably, mounting evidence points to necroptosis as an essential factor associated with ischemic cardiac injury [34–39]. Nevertheless, the landscape of necroptosis genes in CHD is ambiguous. Therefore, this study aimed to recognize and filter necroptosis-related genes that might be diagnostic markers for CHD based on public databases using bioinformatics techniques and to reveal their potential molecular mechanisms.

In the present study, we obtained a total of 94 DE-NRGs based on the GSE20681 dataset by ssGSEA, WGCNA, and DEG analysis. GO-BP analysis revealed that these DE-NRGs were significantly enriched in 'regulation of mitochondrial outer membrane permeabilization involved in apoptotic signaling pathway', 'mitochondrial outer membrane permeabilization', 'positive regulation of mitochondrial membrane permeability involved in apoptotic process', 'mitochondrial outer membrane permeabilization involved in programmed cell death', 'positive regulation of mitochondrial membrane permeability', 'regulation of mitochondrial membrane permeability involved in apoptotic process', and 'regulation of mitochondrial membrane permeability'. Interestingly, the crucial for regulating necroptosis in cardiomyocytes subjected to diverse stimuli, investigations already demonstrate, is the receptor-interacting protein 3-(RIPK3-) mediated mitochondrial permeability transition pore (mPTP) opening signaling pathway [34,40,41]. More precisely, the opening of mTPPs triggers the dissipation of the proton gradient, which in turn modulates oxidative phosphorylation and ATP synthesis, leading to mitochondrial swelling and eventually rupture. This chain of events ultimately results in cardiomyocyte necroptosis [42,43]. The results of our analysis seemed to indirectly demonstrate the involvement of DE-NRG in the process of CHD by regulating mitochondrial permeability to induce cardiomyocyte apoptosis. Normally, cardiomyocytes have a wealth of endoplasmic reticulum (ER) that is necessary for contractile and metabolic processes [44,45]. Consequently, cardiomyocytes would be extremely vulnerable to endoplasmic reticulum stress (ERS) induced by exogenous injury (e.g., ischemia and hypoxia), leading to cell death [45].

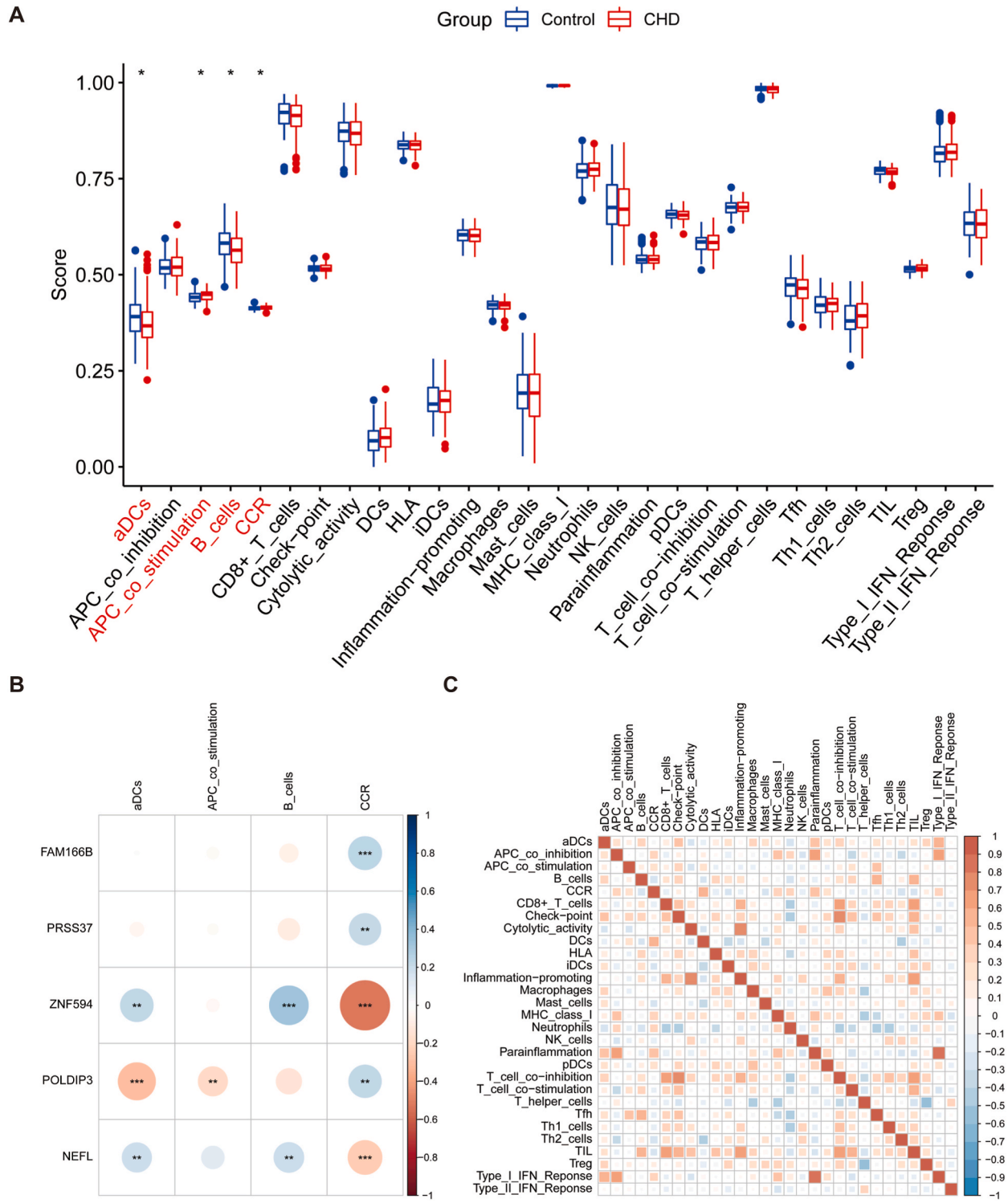

Fig. 6. Analysis and visualization of immune cell infiltration A. Comparison of the ssGSEA scores of 13 immune-related functions and 16 immune cells between the CHD and normal groups. B. Heat map of the correlation of five necroptosis-related biomarkers with four differentially expressed immune elements. C. Correlation heatmap showing the association of various immune cell subsets. $^{*}P < 0.05$; $^{**}P < 0.01$; $^{***}P < 0.001$. ssGSEA, single-sample gene set enrichment analysis; CHD, coronary heart disease.

Table 6
Correlation of 5 necroptosis-related biomarkers with the differential abundance of immune elements.

immune_cells	gene	cor	p.value
aDCs	FAM166B	−0.05	0.45
aDCs	PRSS37	−0.034	0.65
aDCs	ZNF594	0.25	0.00
aDCs	POLDIP3	−0.34	0.00
aDCs	NEFL	0.19	0.01
APC_co_stimulation	FAM166B	−0.09	0.23
APC_co_stimulation	PRSS37	−0.04	0.57
APC_co_stimulation	ZNF594	−0.01	0.94
APC_co_stimulation	POLDIP3	−0.18	0.01
APC_co_stimulation	NEFL	0.10	0.15
B_cells	FAM166B	−0.06	0.42
B_cells	PRSS37	−0.13	0.07
B_cells	ZNF594	0.31	0.00
B_cells	POLDIP3	−0.13	0.06
B_cells	NEFL	0.18	0.01
CCR	FAM166B	0.19	0.01
CCR	PRSS37	0.24	0.00
CCR	ZNF594	−0.51	0.00
CCR	POLDIP3	0.23	0.00
CCR	NEFL	−0.26	0.00

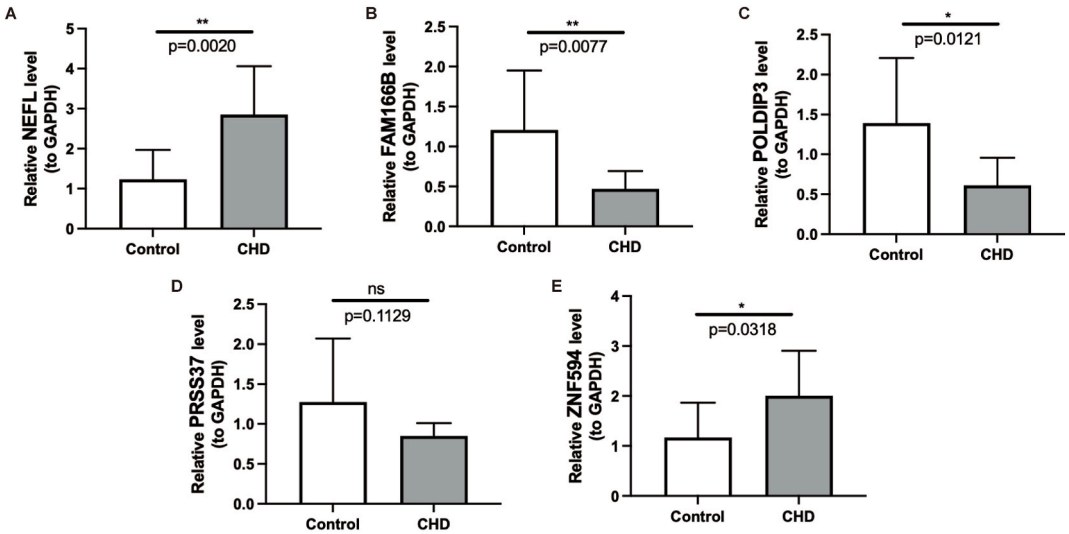

Fig. 7. mRNA expression of necroptosis-related biomarkers qRT-PCR validation of the expression of NEFL (A), FAM166B (B), POLDIP3 (C), PRSS37 (D), and ZNF594 (E) in 10 pairs of CHD and healthy samples. *$P < 0.05$, **$P < 0.01$, and ns $P > 0.05$. qRT-PCR, quantitative real-time polymerase chain reaction; CHD, coronary heart disease.

Consistently, GO-BP analysis revealed that DE-NRGs were intimately tied to ERS responses ('negative regulation of response to endoplasmic reticulum stress' and 'regulation of response to endoplasmic reticulum stress'), ERS-induced apoptotic pathways ('negative regulation of endoplasmic reticulum stress-induced intrinsic apoptotic signaling pathway', 'regulation of endoplasmic reticulum stress-induced intrinsic apoptotic signaling pathway', and 'intrinsic apoptotic signaling pathway in response to endoplasmic reticulum stress'), and 'endoplasmic reticulum membrane organization'. Meanwhile, researchers have demonstrated that ERS inhibition improves cardiac function and reduces adverse remodeling and cardiac apoptosis [46,47]. Accordingly, these results implied that controlling DE-NRGs-regulated ERS and downstream necroptosis holds promise as an important route to retard CHD progression.

Subsequently, the five true signature genes, family with sequence similarity 166 member B (*FAM166B*), neurofilament light chain (*NEFL*), DNA polymerase delta interacting protein 3 (*POLDIP3*), serine protease 37 (*PRSS37*), and zinc finger protein 594 (*ZNF594*), filtered by intersecting two machine learning algorithms (LASSO and SVM-RFE), proceeded to undergo ROC analysis to identify necroptosis-related biomarkers. Although the independent ROC results for the above 5 genes were not satisfactory (all AUC <0.6), the 5-gene-based linear regression model exhibited acceptable power in differentiating CHD from healthy control samples (AUC = 0.75). Moreover, considering the lack of exploration of necroptosis gene profiles in CHD, we considered the above-mentioned 5 true signature genes as potential diagnostic necroptosis-related biomarkers for CHD.

With our knowledge, all the above five necroptosis-related biomarkers are protein-coding genes and are the first to be assigned

significance as diagnostic markers for CHD. By reviewing the available literature, it was found that increased *FAM166B* expression relates to a favorable prognosis in breast cancer (BRCA) and is likely to be an independent prognostic factor [48]. Besides, this gene was shown to be significantly upregulated (3.693-fold) in multiple symmetric lipomatosis (MSL) [49]. Presently, perturbations of *NEFL* have been documented as a trigger for motor neuron diseases (e.g. Charcot-Marie-Tooth) [50,51]. Except for affecting the nervous system, *NEFL* is also recognized as a tumor suppressor, and its loss of heterozygosity (LOH) is relevant to the carcinogenic effect of several cancers (BRCA, colorectal cancer, prostate cancer, etc.) [52–54]. Until now, studies related to *POLDIP3* have emphasized its involvement in the development of neurological diseases (amyotrophic lateral sclerosis) [55], immune diseases (systemic vasculitis) [56], and carcinomas (colorectal adenocarcinoma, hepatocellular carcinoma, gastric carcinoma, etc.) [57–59]. Previously, *PRSS37*, also known as *TRYX2*, was identified as one of the potential genes associated with increased susceptibility to colorectal cancer. The identification was based on the occurrence of rare mutations resulting in premature protein truncation in two or three families affected by the disease [60]. More commonly, however, studies related to this gene have centered on male infertility [61,62]. Previous studies have revealed that one of the zinc finger genes, *ZNF594*, is strongly connected with airway remodeling in asthma patients [63]. Furthermore, it has been hypothesized that *ZNF594* may influence the usefulness of inhaled 2-adrenergic receptor agonists in the treatment of asthma [64]. A recent study suggested that the *ZNF594* variant may be a new genetic marker for prothrombin time (PT) [65].

As mentioned previously, the molecular mechanisms of these necroptosis-related biomarkers in CHD progression remain ambiguous. Therefore, we utilized GSEA for each biomarker to reveal their underlying molecular mechanisms. In the present study, we concentrated on the GO-BP terminology and KEGG pathway that were co-enriched by the five biomarkers. In the GO-BP analysis, we noticed that blood circulation-related terms were significantly enriched. CHD is caused by plaque aggregation in the coronary artery wall. As plaque continues to accumulate, the lumen of the artery continues to narrow, which can lead to partial or complete blood circulation impairment and eventually induce angina pectoris, myocardial infarction, and heart failure [66]. Therefore, improving blood circulation may achieve the reversal of damaged heart function. Meanwhile, these biomarkers were also tightly linked to biological processes related to membrane potential, catecholamine secretion, and calcium ion (Ca^{2+}) homeostasis. Conclusive evidence is that the inward transmembrane flow of Ca^{2+} is an integral part of myocardial action potential formation. Then, as an intracellular messenger, Ca^{2+} binds to troponin in the myocardium and activates the contractile process. Therefore, Ca^{2+} plays an extremely important role in the excitation-contraction coupling process of the myocardium [67–69]. Besides, investigations have illustrated that catecholamines can generate membrane potential oscillations characteristic of post-depolarization by enhancing Ca^{2+} currents and consequent sodium-calcium ion exchange, which may be related to the development of atrial fibrillation [70]. Notably, the 'mitochondrial gene expression', 'mitochondrial translation', and 'mitochondrial ATP synthesis coupled electron transport' were also the five biomarkers commonly enriched to BP terms. Studies have indicated that mitochondria are the engine that drives cardiac pumping and plays a key role in the development and progression of various types of heart disease [71,72]. Moreover, mitochondrial dysfunction is widely recognized as an important cause of necrotic and apoptotic cell death, while Ca^{2+} treatment contributes to mitochondrial dysfunction and mPTP opening [73,74]. Combined with the previous discussion, the opening of mPTP is a critical mechanism leading to cardiomyocyte necroptosis. Therefore, the above evidence hinted that the identified necroptosis-related biomarkers may affect mPTP opening by regulating Ca^{2+} homeostasis, catecholamine secretion, and mitochondria-related biological processes, which could control necroptosis of cardiac myocytes and thus influence the course of CHD. Furthermore, five biomarkers co-involved in the KEGG pathway, such as the 'cAMP signaling pathway', 'Calcium signaling pathway' [75–77], and 'Ras signaling pathway' [78–80], have been extensively studied to demonstrate their robust association with cardiac disease. Therefore, selective targeting of these pathways could serve as an innovative approach to developing necroptosis gene therapy in heart disease.

Accumulating evidence suggests that immune cell infiltration may play a decisive role in the pathology of CHD [81] and, perhaps, that some immune changes are already existing before observable pathology [82]. Therefore, assessment of immune cell infiltration is important to elucidate the molecular mechanisms behind CHD [83]. The results indicated that antigen-presenting cell (APC) co-stimulation and CC chemokine receptor (CCR) abundance were significantly higher in the CHD group (both $P < 0.05$). The inflammatory response of concern in CHD treatment in recent years has been evidenced throughout the initiation & progression of atherosclerosis (AS; the main cause of CHD) and plaque rupture and thrombosis [84], while APC is involved in the inflammatory response to AS [85]. Meantime, it has been established that immune cells rely on co-stimulation in the presence of APC to activate the immune response [86,87]. Such evidence might corroborate that AS may be the result of the interaction between inflammation and the immune system [88]. Chemokines are a small, highly basic family of proteins that includes four subfamilies (i.e., C, CC, CXC, and CX3C) [89,90]. CCRs are mainly expressed by T cells and monocyte-macrophages and are relevant to chronic inflammation [91]. The interaction of chemokines and CCR stimulates the migration of lymphocytes, neutrophils, and endothelial cells and influences angiogenesis and metastasis [92]. Genes encoding CCRs, such as CCR2 and CCR5, have been proposed as genetic hallmarks of coronary artery disease [93,94]. In addition, cumulative studies suggest that high expression of CC-Chemokine Ligand 2 (CCL2) in CHD patients is strongly correlated with poor cardiac outcomes and high persistent mortality [95,96]. Our results also provide a theoretical basis for an increased abundance of APC and CCR causing AS progression and driving CHD development. Furthermore, the reduced infiltration of activated dendritic cells (aDCs) and B cells (both $P < 0.05$) in the CHD group were APCs, of which DCs were the most effective specialized APCs. Currently, both DCs and B cells are considered to play a key role in atherogenesis and may be valuable therapeutic modalities for the prevention of cardiovascular disease [97,98]. In contrast to our results, studies have shown an increase in the number of DCs in the early development of atherosclerotic lesions [99], and similar studies are available for the expression of B cells [100,101]. We regarded the immune microenvironment as a double-edged sword that can both promote the progression of cardiac disease and take a critical part in cardiac injury repair. Recent findings suggest that dendritic cells (DCs) play a key role in regulating the recruitment of monocytes and macrophages during the repair of cardiac injury. Moreover, the recruitment of eosinophils and mast

cells has been associated with the release of biological mediators that contribute to coronary vasoconstriction, as well as leukocyte recruitment. On the other hand, B cells appear to have a protective effect against myocardial injury by preserving cardiac function during the resolution of inflammation, and by regulating wound healing and tissue remodeling after myocardial injury [102]. Meanwhile, the level of immune cell infiltration should be dynamic during the disease process. Inspired by this, we speculated here that the reduced abundance of aDCs and B cells might be correlated with the organism's autonomous repair while leaving these two immune cells depleted, however, the mechanisms underlying this need to be investigated and confirmed further.

In this study, we have screened the critical necroptosis-related genes for CHD. Our findings unveiled the robust predictive capability of the biomarker-based model and initially explored the potential mechanisms of these diagnostic markers in CHD, also capturing the correlation with immune infiltration. However, several limitations of this study should also be noticed. First, our results relied on a public dataset, which could restrict the predictive ability of the filtered genes and the constructed model, and new evidence from future studies may update the current results. Second, qRT-PCR analysis in clinical samples detected genes with expression trends opposite to the bioinformatics analysis results. This was probably related to sample size, ethnicity, and disease status. It was suggested that follow-up studies should expand the sample size and compare the effect of baseline characteristics such as ethnicity and disease status on biomarker expression. Finally, our study was the first to explore necroptosis-related genes in CHD, and the analysis was mainly based on public databases, so further studies will be needed to investigate the detailed molecular mechanisms.

5. Conclusion

In this study, we identified five differentially expressed necroptosis-related genes in CHD using combined WGCNA, LASSO, and SVM-RFE approaches, and developed a linear regression model with satisfactory diagnostic power. Our findings have significant implications for CHD diagnosis and understanding its pathogenesis. The proposed diagnostic model may accurately diagnose CHD in clinical settings and inform personalized treatment strategies. In conclusion, this study provides robust support for CHD diagnosis and treatment, laying a foundation for future research in related fields.

Data availability statement

GSE20681 dataset analyzed in this study was collected from the Gene Expression Omnibus (GEO) database (http://www.ncbi.nlm.nih.gov/geo/). The necroptosis genes were sourced from the Kyoto Encyclopedia of Genes and Genomes (KEGG) database. Further inquiries can be directed to the corresponding author/s.

Funding

None.

CRediT authorship contribution statement

Hongjun You: Writing – review & editing, Writing – original draft, Visualization, Validation, Supervision, Software, Resources, Project administration, Methodology, Investigation, Formal analysis, Data curation, Conceptualization. **Wenqi Han:** Writing – review & editing, Writing – original draft, Visualization, Validation, Supervision, Software, Resources, Project administration, Methodology, Investigation, Formal analysis, Data curation, Conceptualization.

Declaration of competing interest

The authors declare that they have no known competing financial interests or personal relationships that could have appeared to influence the work reported in this paper.

Acknowledgements

None.

Appendix A. Supplementary data

Supplementary data to this article can be found online at https://doi.org/10.1016/j.heliyon.2024.e30269.

References

[1] A. Cassar, D.R. Holmes Jr., C.S. Rihal, B.J. Gersh, Chronic coronary artery disease: diagnosis and management, Mayo Clin. Proc. 84 (2009) 1130–1146, https://doi.org/10.4065/mcp.2009.0391.

[2] F. Liang, Y. Wang, Coronary heart disease and atrial fibrillation: a vicious cycle, Am. J. Physiol. Heart Circ. Physiol. 320 (2021) H1–h12, https://doi.org/10.1152/ajpheart.00702.2020.

[3] Report on Cardiovascular Health and Diseases in China 2021, An updated summary, Biomed. Environ. Sci. 35 (2022) 573–603, https://doi.org/10.3967/bes2022.079.

[4] S.S. Virani, A. Alonso, H.J. Aparicio, E.J. Benjamin, M.S. Bittencourt, C.W. Callaway, et al., Heart disease and stroke statistics-2021 update: a Report from the American heart association, Circulation 143 (2021) e254–e743, https://doi.org/10.1161/cir.0000000000000950.

[5] J. Knuuti, W. Wijns, A. Saraste, D. Capodanno, E. Barbato, C. Funck-Brentano, et al., ESC Guidelines for the diagnosis and management of chronic coronary syndromes, Eur. Heart J. 41 (2020) (2019) 407–477, https://doi.org/10.1093/eurheartj/ehz425.

[6] G.W. Stone, J.F. Sabik, P.W. Serruys, C.A. Simonton, P. Généreux, J. Puskas, et al., Everolimus-eluting stents or bypass surgery for left main coronary artery disease, N. Engl. J. Med. 375 (2016) 2223–2235, https://doi.org/10.1056/NEJMoa1610227.

[7] L.M. Baudhuin, Genetics of coronary artery disease: focus on genome-wide association studies, Am. J. Transl. Res. 1 (2009) 221–234.

[8] A. Linkermann, D.R. Green, Necroptosis, N. Engl. J. Med. 370 (2014) 455–465, https://doi.org/10.1056/NEJMra1310050.

[9] X. Liu, X. Xie, Y. Ren, Z. Shao, N. Zhang, L. Li, et al., The role of necroptosis in disease and treatment, MedComm. 2 (2021) (2020) 730–755, https://doi.org/10.1002/mco2.108.

[10] S. Li, L.G. Ning, X.H. Lou, G.Q. Xu, Necroptosis in inflammatory bowel disease and other intestinal diseases, World J. Clin. Cases 6 (2018) 745–752, https://doi.org/10.12998/wjcc.v6.i14.745.

[11] K. Gupta, N. Phan, Q. Wang, B. Liu, Necroptosis in cardiovascular disease - a new therapeutic target, J. Mol. Cell. Cardiol. 118 (2018) 26–35, https://doi.org/10.1016/j.yjmcc.2018.03.003.

[12] S. Zhe-Wei, G. Li-Sha, L. Yue-Chun, The role of necroptosis in cardiovascular disease, Front. Pharmacol. 9 (2018) 721, https://doi.org/10.3389/fphar.2018.00721.

[13] X. Guo, Y. Chen, Q. Liu, Necroptosis in heart disease: molecular mechanisms and therapeutic implications, J. Mol. Cell. Cardiol. 169 (2022) 74–83, https://doi.org/10.1016/j.yjmcc.2022.05.006.

[14] M. Pasparakis, P. Vandenabeele, Necroptosis and its role in inflammation, Nature 517 (2015) 311–320, https://doi.org/10.1038/nature14191.

[15] S. Hänzelmann, R. Castelo, J. Guinney, GSVA: gene set variation analysis for microarray and RNA-seq data, BMC Bioinf. 14 (2013) 7, https://doi.org/10.1186/1471-2105-14-7.

[16] P. Langfelder, S. Horvath, WGCNA: an R package for weighted correlation network analysis, BMC Bioinf. 9 (2008) 559, https://doi.org/10.1186/1471-2105-9-559.

[17] L. Chen, L. Yuan, K. Qian, G. Qian, Y. Zhu, C.L. Wu, et al., Identification of biomarkers associated with pathological stage and prognosis of clear cell renal cell carcinoma by Co-expression network analysis, Front. Physiol. 9 (2018) 399, https://doi.org/10.3389/fphys.2018.00399.

[18] M.E. Ritchie, B. Phipson, D. Wu, Y. Hu, C.W. Law, W. Shi, et al., Limma powers differential expression analyses for RNA-sequencing and microarray studies, Nucleic Acids Res. 43 (2015) e47, https://doi.org/10.1093/nar/gkv007.

[19] K. Ito, D. Murphy, Application of ggplot2 to pharmacometric graphics, CPT Pharmacometrics Syst. Pharmacol. 2 (2013) e79, https://doi.org/10.1038/psp.2013.56.

[20] X. Zhang, P. Chao, L. Zhang, L. Xu, X. Cui, S. Wang, et al., Single-cell RNA and transcriptome sequencing profiles identify immune-associated key genes in the development of diabetic kidney disease, Front. Immunol. 14 (2023) 1030198, https://doi.org/10.3389/fimmu.2023.1030198.

[21] P. Bardou, J. Mariette, F. Escudié, C. Djemiel, C. Klopp jvenn, An interactive Venn diagram viewer, BMC Bioinf. 15 (2014) 293, https://doi.org/10.1186/1471-2105-15-293.

[22] G. Yu, L.G. Wang, Y. Han, Q.Y. He, clusterProfiler: an R package for comparing biological themes among gene clusters, OMICS 16 (2012) 284–287, https://doi.org/10.1089/omi.2011.0118.

[23] T. Wu, E. Hu, S. Xu, M. Chen, P. Guo, Z. Dai, et al., clusterProfiler 4.0: a universal enrichment tool for interpreting omics data, Innovation 2 (2021) 100141, https://doi.org/10.1016/j.xinn.2021.100141.

[24] Y. Antonacci, J. Toppi, D. Mattia, A. Pietrabissa, L. Astolfi, Single-trial connectivity estimation through the least absolute shrinkage and selection operator, Annu. Int. Conf. IEEE Eng. Med. Biol. Soc. 2019 (2019) 6422–6425, https://doi.org/10.1109/embc.2019.8857909.

[25] H. Sanz, C. Valim, E. Vegas, J.M. Oller, F. Reverter, SVM-RFE: selection and visualization of the most relevant features through non-linear kernels, BMC Bioinf. 19 (2018) 432, https://doi.org/10.1186/s12859-018-2451-4.

[26] H. Chen, J. Zhang, X. Sun, Y. Wang, Y. Qian, Mitophagy-mediated molecular subtypes depict the hallmarks of the tumour metabolism and guide precision chemotherapy in pancreatic adenocarcinoma, Front. Cell Dev. Biol. 10 (2022) 901207, https://doi.org/10.3389/fcell.2022.901207.

[27] M.S. Rooney, S.A. Shukla, C.J. Wu, G. Getz, N. Hacohen, Molecular and genetic properties of tumors associated with local immune cytolytic activity, Cell 160 (2015) 48–61, https://doi.org/10.1016/j.cell.2014.12.033.

[28] K.J. Livak, T.D. Schmittgen, Analysis of relative gene expression data using real-time quantitative PCR and the 2(-Delta Delta C(T)) Method, Methods 25 (2001) 402–408, https://doi.org/10.1006/meth.2001.1262.

[29] regional Global, National age-sex specific all-cause and cause-specific mortality for 240 causes of death, 1990-2013: a systematic analysis for the Global Burden of Disease Study 2013, Lancet 385 (2015) 117–171, https://doi.org/10.1016/s0140-6736(14)61682-2.

[30] H. Wang, Z. Liu, J. Shao, L. Lin, M. Jiang, L. Wang, et al., Immune and inflammation in acute coronary syndrome: molecular mechanisms and therapeutic implications, J. Immunol. Res. 2020 (2020) 4904217, https://doi.org/10.1155/2020/4904217.

[31] P.M. Ridker, From CANTOS to CIRT to COLCOT to clinic: will all atherosclerosis patients soon Be treated with combination lipid-lowering and inflammation-inhibiting agents? Circulation 141 (2020) 787–789, https://doi.org/10.1161/circulationaha.119.045256.

[32] G.A. Roth, M.D. Huffman, A.E. Moran, V. Feigin, G.A. Mensah, M. Naghavi, et al., Global and regional patterns in cardiovascular mortality from 1990 to 2013, Circulation 132 (2015) 1667–1678, https://doi.org/10.1161/circulationaha.114.008720.

[33] M. Samuel, J.C. Tardif, N. Bouabdallaoui, P. Khairy, M.P. Dubé, L. Blondeau, et al., Colchicine for secondary prevention of cardiovascular disease: a systematic review and meta-analysis of randomized controlled trials, Can. J. Cardiol. 37 (2021) 776–785, https://doi.org/10.1016/j.cjca.2020.10.006.

[34] T. Zhang, Y. Zhang, M. Cui, L. Jin, Y. Wang, F. Lv, et al., CaMKII is a RIP3 substrate mediating ischemia- and oxidative stress-induced myocardial necroptosis, Nat. Med. 22 (2016) 175–182, https://doi.org/10.1038/nm.4017.

[35] C.C. Smith, S.M. Davidson, S.Y. Lim, J.C. Simpkin, J.S. Hothersall, D.M. Yellon, Necrostatin: a potentially novel cardioprotective agent? Cardiovasc. Drugs Ther. 21 (2007) 227–233, https://doi.org/10.1007/s10557-007-6035-1.

[36] Y.R. Liu, H.M. Xu, Protective effect of necrostatin-1 on myocardial tissue in rats with acute myocardial infarction, Genet. Mol. Res. 15 (2016), https://doi.org/10.4238/gmr.15027298.

[37] M.I. Oerlemans, J. Liu, F. Arslan, K. den Ouden, B.J. van Middelaar, P.A. Doevendans, et al., Inhibition of RIP1-dependent necrosis prevents adverse cardiac remodeling after myocardial ischemia-reperfusion in vivo, Basic Res. Cardiol. 107 (2012) 270, https://doi.org/10.1007/s00395-012-0270-8.

[38] M. Luedde, M. Lutz, N. Carter, J. Sosna, C. Jacoby, M. Vucur, et al., RIP3, a kinase promoting necroptotic cell death, mediates adverse remodelling after myocardial infarction, Cardiovasc. Res. 103 (2014) 206–216, https://doi.org/10.1093/cvr/cvu146.

[39] S.Y. Lim, S.M. Davidson, M.M. Mocanu, D.M. Yellon, C.C. Smith, The cardioprotective effect of necrostatin requires the cyclophilin-D component of the mitochondrial permeability transition pore, Cardiovasc. Drugs Ther. 21 (2007) 467–469, https://doi.org/10.1007/s10557-007-6067-6.

[40] G. Kung, K. Konstantinidis, R.N. Kitsis, Programmed necrosis, not apoptosis, in the heart, Circ. Res. 108 (2011) 1017–1036, https://doi.org/10.1161/circresaha.110.225730.

[41] P. Zhu, S. Hu, Q. Jin, D. Li, F. Tian, S. Toan, et al., Ripk3 promotes ER stress-induced necroptosis in cardiac IR injury: a mechanism involving calcium overload/XO/ROS/mPTP pathway, Redox Biol. 16 (2018) 157–168, https://doi.org/10.1016/j.redox.2018.02.019.

[42] S.Y. Lim, D.J. Hausenloy, S. Arjun, A.N. Price, S.M. Davidson, M.F. Lythgoe, et al., Mitochondrial cyclophilin-D as a potential therapeutic target for post-myocardial infarction heart failure, J. Cell Mol. Med. 15 (2011) 2443–2451, https://doi.org/10.1111/j.1582-4934.2010.01235.x.

[43] H. Zhou, D. Li, P. Zhu, Q. Ma, S. Toan, J. Wang, et al., Inhibitory effect of melatonin on necroptosis via repressing the Ripk3-PGAM5-CypD-mPTP pathway attenuates cardiac microvascular ischemia-reperfusion injury, J. Pineal Res. 65 (2018) e12503, https://doi.org/10.1111/jpi.12503.

[44] C.D. Ochoa, R.F. Wu, L.S. Terada, ROS signaling and ER stress in cardiovascular disease, Mol. Aspect. Med. 63 (2018) 18–29, https://doi.org/10.1016/j.mam.2018.03.002.

[45] L. Chang, Z. Wang, F. Ma, B. Tran, R. Zhong, Y. Xiong, et al., ZYZ-803 mitigates endoplasmic reticulum stress-related necroptosis after acute myocardial infarction through downregulating the RIP3-CaMKII signaling pathway, Oxid. Med. Cell. Longev. 2019 (2019) 6173685, https://doi.org/10.1155/2019/6173685.

[46] T. Luo, J.K. Kim, B. Chen, A. Abdel-Latif, M. Kitakaze, L. Yan, Attenuation of ER stress prevents post-infarction-induced cardiac rupture and remodeling by modulating both cardiac apoptosis and fibrosis, Chem. Biol. Interact. 225 (2015) 90–98, https://doi.org/10.1016/j.cbi.2014.10.032.

[47] Z.Y. Shi, Y. Liu, L. Dong, B. Zhang, M. Zhao, W.X. Liu, et al., Cortistatin improves cardiac function after acute myocardial infarction in rats by suppressing myocardial apoptosis and endoplasmic reticulum stress, J. Cardiovasc. Pharmacol. Therapeut. 22 (2017) 83–93, https://doi.org/10.1177/1074248416644988.

[48] W. Hu, M. Li, Q. Zhang, C. Liu, X. Wang, J. Li, et al., Establishment of a novel CNV-related prognostic signature predicting prognosis in patients with breast cancer, J. Ovarian Res. 14 (2021) 103, https://doi.org/10.1186/s13048-021-00823-y.

[49] K. Chen, L. Wang, W. Yang, C. Wang, G. Hu, Z. Mo, Profiling of differentially expressed genes in adipose tissues of multiple symmetric lipomatosis, Mol. Med. Rep. 16 (2017) 6570–6579, https://doi.org/10.3892/mmr.2017.7437.

[50] R.K. Liem, S.H. Yen, G.D. Salomon, M.L. Shelanski, Intermediate filaments in nervous tissues, J. Cell Biol. 79 (1978) 637–645, https://doi.org/10.1083/jcb.79.3.637.

[51] I.V. Mersiyanova, A.V. Perepelov, A.V. Polyakov, V.F. Sitnikov, E.L. Dadali, R.B. Oparin, et al., A new variant of Charcot-Marie-Tooth disease type 2 is probably the result of a mutation in the neurofilament-light gene, Am. J. Hum. Genet. 67 (2000) 37–46, https://doi.org/10.1086/302962.

[52] A. Imbert, M. Chaffanet, L. Essioux, T. Noguchi, J. Adélaïde, F. Kerangueven, et al., Integrated map of the chromosome 8p12-p21 region, a region involved in human cancers and Werner syndrome, Genomics 32 (1996) 29–38, https://doi.org/10.1006/geno.1996.0073.

[53] J.A. Macoska, T.M. Trybus, P.D. Benson, W.A. Sakr, D.J. Grignon, K.D. Wojno, et al., Evidence for three tumor suppressor gene loci on chromosome 8p in human prostate cancer, Cancer Res. 55 (1995) 5390–5395.

[54] F. Lerebours, S. Olschwang, B. Thuille, A. Schmitz, P. Fouchet, P. Laurent-Puig, et al., Deletion mapping of the tumor suppressor locus involved in colorectal cancer on chromosome band 8p21, Genes Chromosomes Cancer 25 (1999) 147–153, https://doi.org/10.1002/(sici)1098-2264(199906)25:2<147::aid-gcc10>3.0.co;2-z.

[55] A. Shiga, T. Ishihara, A. Miyashita, M. Kuwabara, T. Kato, N. Watanabe, et al., Alteration of POLDIP3 splicing associated with loss of function of TDP-43 in tissues affected with ALS, PLoS One 7 (2012) e43120, https://doi.org/10.1371/journal.pone.0043120.

[56] J. Avila, E. Acosta, M.D. Machargo, M.F. Arteaga, E. Gallego, H. Cañete, et al., Autoantigenic nuclear proteins of a clinically atypical renal vasculitis, J. Autoimmune Dis. 5 (2008) 3, https://doi.org/10.1186/1740-2557-5-3.

[57] S. Lou, F. Meng, X. Yin, Y. Zhang, B. Han, Y. Xue, Comprehensive characterization of RNA processing factors in gastric cancer identifies a prognostic signature for predicting clinical outcomes and therapeutic responses, Front. Immunol. 12 (2021) 719628, https://doi.org/10.3389/fimmu.2021.719628.

[58] X.N. Liu, J.H. Yuan, T.T. Wang, W. Pan, S.H. Sun, An alternative POLDIP3 transcript promotes hepatocellular carcinoma progression, Biomed. Pharmacother. 89 (2017) 276–283, https://doi.org/10.1016/j.biopha.2017.01.139.

[59] X. Wang, S. Zhang, R. Zheng, F. Yue, S.H. Lin, A.A. Rahmeh, et al., PDIP46 (DNA polymerase δ interacting protein 46) is an activating factor for human DNA polymerase δ, Oncotarget 7 (2016) 6294–6313, https://doi.org/10.18632/oncotarget.7034.

[60] A.E. Gylfe, R. Katainen, J. Kondelin, T. Tanskanen, T. Cajuso, U. Hänninen, et al., Eleven candidate susceptibility genes for common familial colorectal cancer, PLoS Genet. 9 (2013) e1003876, https://doi.org/10.1371/journal.pgen.1003876.

[61] J. Liu, C. Shen, W. Fan, Y. Chen, A. Zhang, Y. Feng, et al., Low levels of PRSS37 protein in sperm are associated with many cases of unexplained male infertility, Acta Biochim. Biophys. Sin. 48 (2016) 1058–1065, https://doi.org/10.1093/abbs/gmw096.

[62] M. Hezavehei, M. Sharafi, R. Fathi, A. Shahverdi, M.A.S. Gilani, Membrane lipid replacement with nano-micelles in human sperm cryopreservation improves post-thaw function and acrosome protein integrity, Reprod. Biomed. Online 43 (2021) 257–268, https://doi.org/10.1016/j.rbmo.2021.05.005.

[63] S. Bazan-Socha, S. Buregwa-Czuma, B. Jakiela, L. Zareba, I. Zawlik, A. Myszka, et al., Reticular basement membrane thickness is associated with growth- and fibrosis-promoting airway transcriptome profile-study in asthma patients, Int. J. Mol. Sci. 22 (2021), https://doi.org/10.3390/ijms22030998.

[64] D. Yan, O. Hamed, T. Joshi, M.M. Mostafa, K.C. Jamieson, R. Joshi, et al., Analysis of the indacaterol-regulated transcriptome in human airway epithelial cells implicates gene expression changes in the adverse and therapeutic effects of β(2)-adrenoceptor agonists, J. Pharmacol. Exp. Therapeut. 366 (2018) 220–236, https://doi.org/10.1124/jpet.118.249292.

[65] F. Zhang, G. Mu, Z. Liu, Q. Xie, H. Zhang, S. Zhou, et al., Genetic polymorphisms associated with prothrombin time and activated partial thromboplastin time in Chinese healthy population, Genes 13 (2022), https://doi.org/10.3390/genes13101867.

[66] G. Heusch, Coronary blood flow in heart failure: cause, consequence and bystander, Basic Res. Cardiol. 117 (2022) 1, https://doi.org/10.1007/s00395-022-00909-8.

[67] A. Fabiato, F. Fabiato, Calcium release from the sarcoplasmic reticulum, Circ. Res. 40 (1977) 119–129, https://doi.org/10.1161/01.res.40.2.119.

[68] J. Lynch, M. Michalak, Ca2+-dependent signaling pathways in the heart: potential drug targets for cardiac disease, Curr. Drug Targets - Cardiovasc. Hematol. Disord. 2 (2002) 1–11, https://doi.org/10.2174/1568006023337853.

[69] C. Montell, The latest waves in calcium signaling, Cell 122 (2005) 157–163, https://doi.org/10.1016/j.cell.2005.07.009.

[70] A.J. Workman, Cardiac adrenergic control and atrial fibrillation, Naunyn-Schmiedeberg's Arch. Pharmacol. 381 (2010) 235–249, https://doi.org/10.1007/s00210-009-0474-0.

[71] E.J. Griffiths, Mitochondria and heart disease, Adv. Exp. Med. Biol. 942 (2012) 249–267, https://doi.org/10.1007/978-94-007-2869-1_11.

[72] C.L. Hoppel, B. Tandler, H. Fujioka, A. Riva, Dynamic organization of mitochondria in human heart and in myocardial disease, Int. J. Biochem. Cell Biol. 41 (2009) 1949–1956, https://doi.org/10.1016/j.biocel.2009.05.004.

[73] L. Azzolin, S. von Stockum, E. Basso, V. Petronilli, M.A. Forte, P. Bernardi, The mitochondrial permeability transition from yeast to mammals, FEBS Lett. 584 (2010) 2504–2509, https://doi.org/10.1016/j.febslet.2010.04.023.

[74] M. Izem-Meziane, B. Djerdjouri, S. Rimbaud, F. Caffin, D. Fortin, A. Garnier, et al., Catecholamine-induced cardiac mitochondrial dysfunction and mPTP opening: protective effect of curcumin, Am. J. Physiol. Heart Circ. Physiol. 302 (2012) H665–H674, https://doi.org/10.1152/ajpheart.00467.2011.

[75] K. Shah, S. Seeley, C. Schulz, J. Fisher, S. Gururaja Rao, Calcium channels in the heart: disease states and drugs, Cells 11 (2022), https://doi.org/10.3390/cells11060943.

[76] E.J. Cartwright, T. Mohamed, D. Oceandy, L. Neyses, Calcium signaling dysfunction in heart disease, Biofactors 37 (2011) 175–181, https://doi.org/10.1002/biof.149.

[77] S. Chakraborti, S. Das, P. Kar, B. Ghosh, K. Samanta, S. Kolley, et al., Calcium signaling phenomena in heart diseases: a perspective, Mol. Cell. Biochem. 298 (2007) 1–40, https://doi.org/10.1007/s11010-006-9355-8.

[78] E.M. Wright, B. Kerr, RAS-MAPK pathway disorders: important causes of congenital heart disease, feeding difficulties, developmental delay and short stature, Arch. Dis. Child. 95 (2010) 724–730, https://doi.org/10.1136/adc.2009.160069.

[79] Y. Zhao, Q. Sun, Z. Xu, M. Li, G. Tian, Effect of ghrelin intervention on the ras/ERK pathway in the regulation of heart failure by PTEN, Comput. Math. Methods Med. 2022 (2022) 1045681, https://doi.org/10.1155/2022/1045681.

[80] B.D. Gelb, M. Tartaglia, RAS signaling pathway mutations and hypertrophic cardiomyopathy: getting into and out of the thick of it, J. Clin. Invest. 121 (2011) 844–847, https://doi.org/10.1172/jci46399.

[81] P. Libby, The changing landscape of atherosclerosis, Nature 592 (2021) 524–533, https://doi.org/10.1038/s41586-021-03392-8.

[82] C.A. Adam, D.L. Șalaru, C. Prisacariu, D.T.M. Marcu, R.A. Sascău, C. Stătescu, Novel biomarkers of atherosclerotic vascular disease-latest insights in the research field, Int. J. Mol. Sci. 23 (2022), https://doi.org/10.3390/ijms23094998.
[83] E. Dounousi, A. Duni, K.K. Naka, G. Vartholomatos, C. Zoccali, The innate immune system and cardiovascular disease in ESKD: monocytes and natural killer cells, Curr. Vasc. Pharmacol. 19 (2021) 63–76, https://doi.org/10.2174/1570161118666200628024027.
[84] C. Weber, H. Noels, Atherosclerosis: current pathogenesis and therapeutic options, Nat. Med. 17 (2011) 1410–1422, https://doi.org/10.1038/nm.2538.
[85] P. Libby, P.M. Ridker, G.K. Hansson, Progress and challenges in translating the biology of atherosclerosis, Nature 473 (2011) 317–325, https://doi.org/10.1038/nature10146.
[86] T.H. Mogensen, Pathogen recognition and inflammatory signaling in innate immune defenses, Clin. Microbiol. Rev. 22 (2009) 240–273, https://doi.org/10.1128/cmr.00046-08. Table of Contents.
[87] M.L. Saiz, V. Rocha-Perugini, F. Sánchez-Madrid, Tetraspanins as organizers of antigen-presenting cell function, Front. Immunol. 9 (2018) 1074, https://doi.org/10.3389/fimmu.2018.01074.
[88] B. Legein, L. Temmerman, E.A. Biessen, E. Lutgens, Inflammation and immune system interactions in atherosclerosis, Cell. Mol. Life Sci. 70 (2013) 3847–3869, https://doi.org/10.1007/s00018-013-1289-1.
[89] I. Clark-Lewis, K.S. Kim, K. Rajarathnam, J.H. Gong, B. Dewald, B. Moser, et al., Structure-activity relationships of chemokines, J. Leukoc. Biol. 57 (1995) 703–711, https://doi.org/10.1002/jlb.57.5.703.
[90] N.G. Frangogiannis, Chemokines in the ischemic myocardium: from inflammation to fibrosis, Inflamm. Res. 53 (2004) 585–595, https://doi.org/10.1007/s00011-004-1298-5.
[91] G.E. White, A.J. Iqbal, D.R. Greaves, CC chemokine receptors and chronic inflammation–therapeutic opportunities and pharmacological challenges, Pharmacol. Rev. 65 (2013) 47–89, https://doi.org/10.1124/pr.111.005074.
[92] Y. Zhong, L. Jiang, H. Lin, B. Li, J. Lan, S. Liang, et al., Expression of CC chemokine receptor 9 predicts poor prognosis in patients with lung adenocarcinoma, Diagn. Pathol. 10 (2015) 101, https://doi.org/10.1186/s13000-015-0341-x.
[93] S. Sharda, A. Gilmour, V. Harris, V.P. Singh, N. Sinha, S. Tewari, et al., Chemokine receptor 5 (CCR5) deletion polymorphism in North Indian patients with coronary artery disease, Int. J. Cardiol. 124 (2008) 254–258, https://doi.org/10.1016/j.ijcard.2006.12.021.
[94] J.K. Pai, P. Kraft, C.C. Cannuscio, J.E. Manson, K.M. Rexrode, C.M. Albert, et al., Polymorphisms in the CC-chemokine receptor-2 (CCR2) and -5 (CCR5) genes and risk of coronary heart disease among US women, Atherosclerosis 186 (2006) 132–139, https://doi.org/10.1016/j.atherosclerosis.2005.06.041.
[95] R.L. Sun, C.X. Huang, J.L. Bao, J.Y. Jiang, B. Zhang, S.X. Zhou, et al., CC-chemokine Ligand 2 (CCL2) suppresses high density lipoprotein (HDL) internalization and cholesterol efflux via CC-chemokine receptor 2 (CCR2) induction and p42/44 mitogen-activated protein kinase (MAPK) activation in human endothelial cells, J. Biol. Chem. 291 (2016) 19532–19544, https://doi.org/10.1074/jbc.M116.714279.
[96] J.A. de Lemos, D.A. Morrow, M.A. Blazing, P. Jarolim, S.D. Wiviott, M.S. Sabatine, et al., Serial measurement of monocyte chemoattractant protein-1 after acute coronary syndromes: results from the A to Z trial, J. Am. Coll. Cardiol. 50 (2007) 2117–2124, https://doi.org/10.1016/j.jacc.2007.06.057.
[97] T. Pattarabanjird, C. Li, C. McNamara, B cells in atherosclerosis: mechanisms and potential clinical applications, JACC Basic Transl. Sci. 6 (2021) 546–563, https://doi.org/10.1016/j.jacbts.2021.01.006.
[98] Y.V. Bobryshev, Dendritic cells and their role in atherogenesis, Lab. Invest. 90 (2010) 970–984, https://doi.org/10.1038/labinvest.2010.94.
[99] Y.V. Bobryshev, R.S. Lord, S-100 positive cells in human arterial intima and in atherosclerotic lesions, Cardiovasc. Res. 29 (1995) 689–696.
[100] E. Ammirati, F. Moroni, M. Magnoni, P.G. Camici, The role of T and B cells in human atherosclerosis and atherothrombosis, Clin. Exp. Immunol. 179 (2015) 173–187, https://doi.org/10.1111/cei.12477.
[101] R. Ding, W. Gao, Z. He, H. Wang, C.D. Conrad, C.M. Dinney, et al., Overrepresentation of Th1- and Th17-like follicular helper T cells in coronary artery disease, J. Cardiovasc. Transl. Res. 8 (2015) 503–505, https://doi.org/10.1007/s12265-015-9662-0.
[102] K. Sun, Y.Y. Li, J. Jin, A double-edged sword of immuno-microenvironment in cardiac homeostasis and injury repair, Signal Transduct. Targeted Ther. 6 (2021) 79, https://doi.org/10.1038/s41392-020-00455-6.